Nile red and DCM fluorescence anisotropy studies in C12E7/DPPC mixed systems

ARTICLE *in* THE JOURNAL OF PHYSICAL CHEMISTRY B · DECEMBER 2002

Impact Factor: 3.3 · DOI: 10.1021/jp026479u

4 AUTHORS, INCLUDING:

Paulo Coutinho
University of Minho
69 PUBLICATIONS **604** CITATIONS
SEE PROFILE

Elisabete M.S. Castanheira
University of Minho
69 PUBLICATIONS **616** CITATIONS
SEE PROFILE

M. Elisabete C.D. Real Oliveira
University of Minho
63 PUBLICATIONS **685** CITATIONS
SEE PROFILE

Nile Red and DCM Fluorescence Anisotropy Studies in $C_{12}E_7$/DPPC Mixed Systems

Paulo J. G. Coutinho,* Elisabete M. S. Castanheira, M. Céu Rei, and M. Elisabete C. D. Real Oliveira

Departamento de Física, Universidade do Minho, Campus de Gualtar, 4710-057 Braga, Portugal

Received: July 9, 2002; In Final Form: October 3, 2002

The lipid/surfactant mixed interactions between the lipid dipalmitoylphosphatydilcholine (DPPC) and the nonionic surfactant $C_{12}E_7$ ($C_{12}H_{25}(OCH_2CH_2)_7OH$) were studied by the use of fluorescence anisotropy of nile red and DCM laser dye. Three different regions consisting of mixed micelles, mixed vesicles, and both aggregates were identified. Nile red fluorescence anisotropy is wavelength-dependent, the spectra being decomposed into two log-normal functions. These results are consistent with a solvent relaxation process, with distinct anisotropies for the relaxed and unrelaxed states. The spectral properties (anisotropy and maximum emission wavelength) of the relaxed state show higher sensitivity to the environment than those of the unrelaxed state. DCM fluorescence anisotropy shows similar trends. This was interpreted as a result of a trans−cis photoisomerization process. The observed anisotropy spectrum was decomposed in two Gaussian functions reflecting a distinct anisotropy for each isomer.

Introduction

Surfactant micelles have the ability to solubilize insoluble or only sparingly soluble materials in aqueous media by incorporating them into the micellar interior with the formation of mixed micelles. Phospholipids and other constituents of biomembranes can also be solubilized by surfactant micelles. Because of this property, surfactants are widely used as molecular tools in membranology.[1] The applications of surfactants in membranology are based on the transformation from vesicles to mixed micelles (or the reverse direction) occurring in aqueous surfactant/phospholipid mixtures.[2,3] An understanding of the transformation phenomenon should be helpful in achieving these practical purposes, and hence great efforts have been developed so far to elucidate the pathway and mechanism of the transformation between vesicles and mixed micelles.[4,5] The surfactant action on the phase transition of vesicle membranes has been studied by the use of several techniques for various surfactant and phospholipid species.[6,7]

Over the entire range of biophysical and spectroscopic methods, several techniques have been used to elucidate the properties of lipid vesicles and vesicle/surfactant interactions: cryotransmission electron microscopy,[4] differential scanning calorimetry,[6] light scattering,[5] and absorption and fluorescence spectroscopy.[8] Fluorescence spectroscopy is probably the technique with the highest sensitivity for the study of lipid vesicles, biomembranes, and lipid/surfactant interactions.

Since lipids are not fluorescent, fluorescence studies of lipid vesicles are made possible by introducing a fluorescence probe into the lipid environment.

The dye nile red (9-(diethylamino)-5H-benzo[α]phenoxazin-5-one) exhibits a hydrophobic nature, with low solubility and fluorescence in water. It has been extensively used to study biological membranes,[9] proteins,[10−12] micelles,[13,14] γ-cyclodextrins,[15] and nonionic surfactant microemulsions.[16] Nile red is a good solvatochromic probe, and both steady-state and time-resolved emission properties are strongly medium-dependent.[17−19]

The compound 4-dicyanomethylene-2-methyl-6-*p*-dimethylaminostyryl-4H-pyran (DCM) is a very efficient laser dye.[20−22] It was found that DCM exists in solution as cis and trans photoisomers[23−25] whose ratio is solvent-dependent,[23] exhibiting a short fluorescence decay time for the cis isomer.[24] The trans → cis photoisomerization relative yields have been determined in several media.[25] The photophysics of DCM has been studied by time-resolved femtosecond absorption spectroscopy[26] and femtosecond Raman spectroscopy.[27] Recently, DCM was used to study the hydrophobic interior of proteins, where this dye has slow solvation dynamics.[28]

In this work, nile red and DCM fluorescence anisotropy are studied in mixed lipid/surfactant systems with several concentration ratios of the phospholipid palmitoylphosphatydilcholine (DPPC) and the nonionic surfactant $C_{12}E_7$ ($C_{12}H_{25}(OCH_2CH_2)_7$-OH).

Experimental Section

Materials. Samples of polyoxyethylene 7 lauryl ether ($C_{12}E_7$) and L-α-dipalmitoylphosphatidylcholine (DPPC) from Sigma

Nile Red

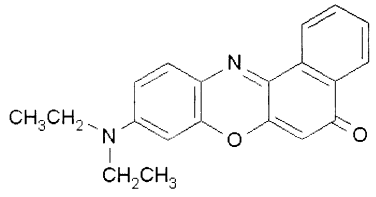

DCM

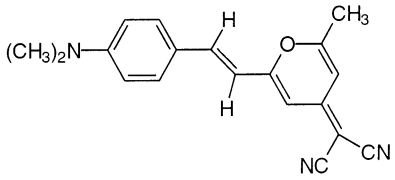

* Corresponding author. E-mail: pcoutinho@fisica.uminho.pt. Tel: +351-253-604-321. Fax: +351-253-678-981.

10.1021/jp026479u CCC: $22.00
Published on Web 00/00/0000 PAGE EST: 6

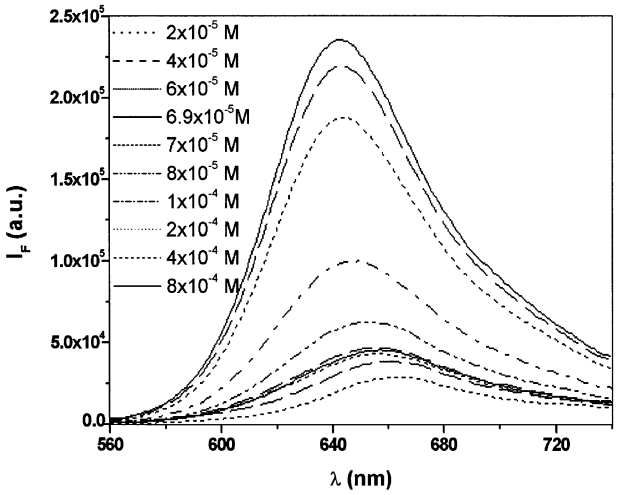

Figure 1. Fluorescence emission spectra of nile red in the $C_{12}E_7$/water system as a function of $C_{12}E_7$ concentration ($\lambda_{exc} = 550$ nm).

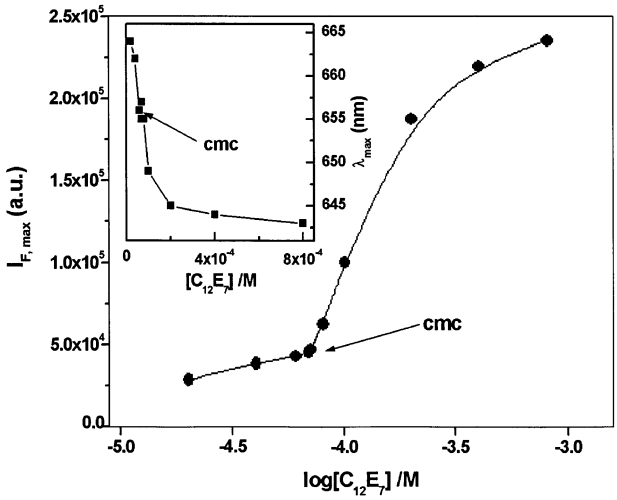

Figure 2. Maximum emission intensity of nile red in the $C_{12}E_7$/water system as a function of $C_{12}E_7$ concentration. The inset shows the maximum emission wavelength of nile red in the $C_{12}E_7$/water system as a function of $C_{12}E_7$ concentration ($\lambda_{exc} = 550$ nm).

were used as received. The solvatochromic probe 9-(diethylamino)-5H-benzo[α]phenoxazin-5-one (nile red) from Aldrich and the laser dye 4-dicyanomethylene-2-methyl-6-*p*-dimethylaminostyryl-4H-pyran (DCM) from Lambda Physik were used as received. Solutions were prepared using Milli-Q-grade water.

Sample Preparation. The samples for the surfactant/water system were prepared by the addition of the required amount of surfactant to water. Fluorescence probes (2×10^{-7} M) were introduced by the injection of 10 μL of a 10^{-4} M stock solution in ethanol. The samples were placed in an ultrasonic bath for mixing and were left to stabilize for at least 1 day. DPPC was deposited by evaporation at 50 °C of a stock solution in ethanol. Then, 5 mL of a 10^{-4} M surfactant solution in water was added, followed by the injection of 10 μL of a 10^{-4} M probe solution in ethanol. The samples were placed in an ultrasonic bath for mixing and were left to stabilize for at least 1 day.

Fluorescence Measurements. Steady-state emission spectra were recorded using a Spex Fluorolog 212 spectrofluorimeter. Polarized emission spectra were recorded using Spex polarizers. The spectra were corrected for the instrumental response of the system.

Results and Discussion

Nile Red in the $C_{12}E_7$/Water System. Before studying the influence of the phospholipid DPPC in mixed phospholipid/$C_{12}E_7$ systems, the behavior of the fluorescent probe nile red was monitored in the surfactant/water system at several surfactant concentrations below and above the critical micelle concentration (cmc) of $C_{12}E_7$ in water (6.9×10^{-5} M).[29]

Figure 1 displays the fluorescence spectra of nile red in the $C_{12}E_7$/water system. It can be seen that the fluorescence intensity rises with increasing surfactant concentration while the maximum emission wavelength exhibits a blue shift.

The cmc value can be seen as the onset of the fluorescence intensity increase (Figure 2). The nile red fluorescence lifetime markedly decreases with the increase in the hydrogen-bonding capability of the medium.[19] This fact explains the sudden rise in fluorescence intensity upon the formation of micelles, as nile red, because of its hydrophobic character, tends to be located in micelles, being more protected from water.

The maximum wavelength of the nile red emission spectrum increases with the polarity of the environment.[17,18] This explains the observed blue shift, as the polarity of the medium surrounding the probe decreases with the rise in $C_{12}E_7$ concentration, and allowed us to locate the cmc value at the inflection point of the wavelength-maximum plot (inset of Figure 2).

The different position of cmc in the plots of fluorescence intensity and emission maximum indicates specific excited-state dynamics of nile red in this microheterogeneous media.

Nile Red in $C_{12}E_7$/DPPC Mixed Systems. In mixed DPPC/$C_{12}E_7$ systems, a surfactant concentration of 10^{-4} M, well above the cmc, was used. In a previous study using pyrene emission,[30] we have been able to detect two different kinds of mixed structures—mixed vesicles and mixed micelles. In the characterization of lipid/micelle interactions, the surfactant molar ratio x_s is usually considered:[7]

$$x_s = \frac{[C_{12}E_7]}{[C_{12}E_7] + [DPPC]} \quad (1)$$

We will consider the usual three-stage model of the solubilization of liposomes by surfactants: mixed vesicles exist up to a critical surfactant concentration, x_{sat}; between x_{sat} and x_{sol}, there are saturated mixed vesicles and saturated mixed micelles with, respectively, x_{sat} and x_{sol} surfactant contents; above x_{sol}, there are only mixed micelles.

Figure 3 displays the maximum emission wavelength for nile red in mixed systems as a function of x_s. This plot clearly evidences the existence of three regions. In previous work using the pyrene excimer-to-monomer emission intensity ratio, a value of x_{sat} near 0.3 could be estimated.[30] Heerklotz et al.[31] obtained an x_{sol} value near 0.75 for the POPC/$C_{12}E_7$ system. In Figure 3, the values of x_{sat} and x_{sol} can be located at the transition points (vertical lines) in the curve near 0.3 and 0.75, in good agreement with previous results.[30, 31]

Figure 4 displays the normalized total emission spectra of nile red (obtained from anisotropy measurements) given by

$$I_{total} = I_{VV} + 2GI_{VH} \quad (2)$$

where I_{VV} and I_{VH} are the emission spectra obtained with vertical

and horizontal polarization, respectively (for excitation with vertical polarized light), and G is the instrumental correction factor given by

$$G = \frac{I_{HV}}{I_{HH}} \tag{3}$$

Besides the expected blue shift with increasing DPPC content (lower x_s) due to the overall decrease in medium polarity, an enlargement in the blue side of the spectrum is readily observed.

The inset of Figure 4 shows that the steady-state anisotropy, r, clearly varies with the emission wavelength, decreasing from a constant value on the blue side to a lower constant value on the red side of the emission spectra. This variation can be explained by two different emitting states of nile red. In fact, nile red excited-state dynamics has been described by a two-state model involving an initially excited state and a solvent relaxed state:[32]

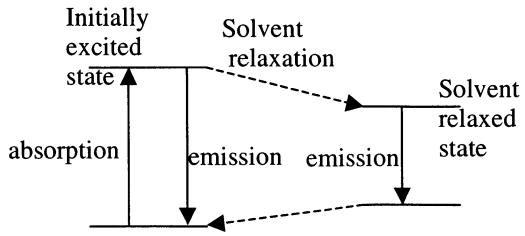

It has been found that the process is viscosity-dependent and is important in SDS micelles, egg−PC vesicles, and high-viscosity alcohols. A consistent dependence of fluorescence lifetime on emission wavelength was also observed.[32]

The observed variations in fluorescence anisotropy with wavelength in DPPC/$C_{12}E_7$ mixtures can be attibuted to different contributions from the two emiting states of nile red.

Each fluorescence anisotropy spectrum of nile red was fitted to a sum of two log-normal functions,[33] one for each emitting state, having the same width and skewness parameters:

$$I_{VV/VH} = \frac{(A_{VV/VH})_1}{(\lambda - (\lambda_{max})_1 + a)} \exp(-c^2) \exp\left\{-\frac{1}{2c^2}\left[\ln\left(\frac{\lambda - (\lambda_{max})_1 + a}{b}\right)\right]^2\right\} + \frac{(A_{VV/VH})_2}{(\lambda - (\lambda_{max})_2 + a)} \exp(-c^2) \exp\left\{-\frac{1}{2c^2}\left[\ln\left(\frac{\lambda - (\lambda_{max})_2 + a}{b}\right)\right]^2\right\} \tag{4}$$

A is the maximum emission intensity at wavelength λ_{max}, and the parameters a, b, and c are given by

$$c = \frac{\ln(\rho)}{\sqrt{2\ln(2)}} \qquad b = H\frac{\rho}{\rho^2 - 1}\exp(c^2) \qquad a = H\frac{\rho}{\rho^2 - 1} \tag{5}$$

where H is the half-width of the band and ρ is its skewness.

The subscript 1 refers to the initially excited state, whereas the subscript 2 refers to the solvent relaxed state.

In Figure 5, a typical fitting is shown.

The steady-state fluorescence anisotropies are then calculated by

$$r_1 = \frac{(A_{VV})_1 - (A_{VH})_1}{(A_{VV})_1 + 2(A_{VH})_1} \quad r_2 = \frac{(A_{VV})_2 - (A_{VH})_2}{(A_{VV})_2 + 2(A_{VH})_2} \tag{6}$$

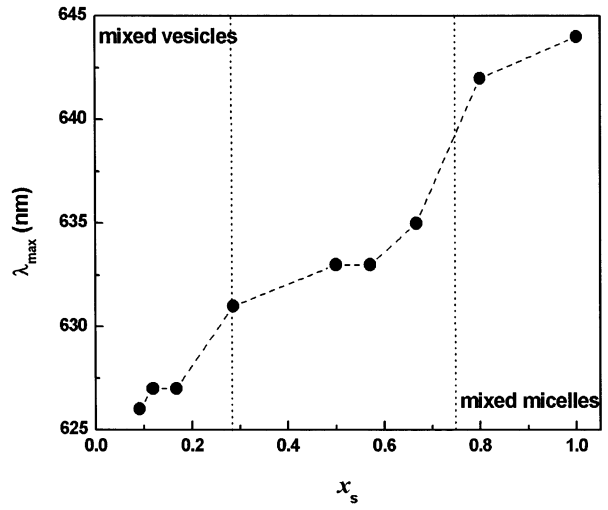

Figure 3. Maximum emission wavelength of nile red in the $C_{12}E_7$/DPPC mixed system (λ_{exc} = 550 nm) as a function of the surfactant molar ratio x_s showing the three regions with mixed vesicles, both mixed vesicles and mixed micelles, and only mixed micelles.

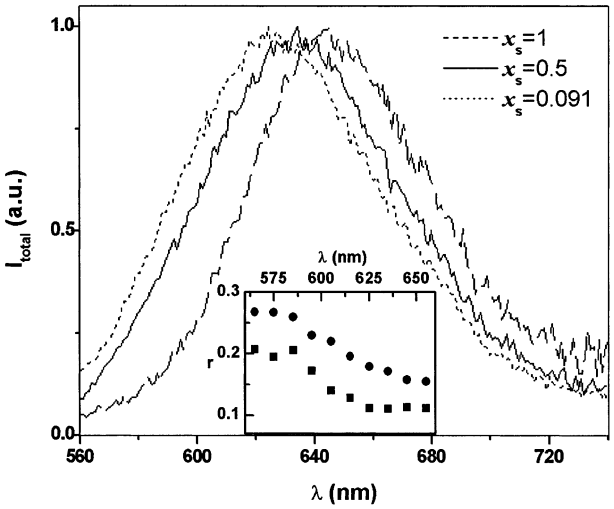

Figure 4. Normalized total-emission spectra ($I_{VV} + 2GI_{VH}$) of nile red for different x_s values (0.091, 0.5, and 1). The inset shows the anisotropy variation with emission wavelength for x_s = 0.67 (●) and 1 (■).

The emission intensity fraction of the initially excited state is

$$f_1 = \frac{(A_{VV})_1 + 2(A_{VH})_1}{(A_{VV})_1 + 2(A_{VH})_1 + (A_{VV})_2 + 2(A_{VH})_2} \tag{7}$$

In Figure 6a, it can be seen that the anisotropy of the initially excited state (1) is higher than that of the relaxed state and is more insensitive to the structure and composition of the mixed aggregate. This is consistent with the published shorter lifetime of the initially excited state of nile red.[32] The anisotropy of the relaxed state rises with DPPC content (decreasing x_s) because of the increase in the local viscosity.

Increasing DPPC content causes a blue shift of the relaxed-state emission (Figure 6b). Bilayer structures (vesicles) usually tend to accommodate guest molecules in their interiors, whereas micelles tend to locate them at the surface.[34]

The contribution from the initially excited state, measured by the fraction f_1 (eq 7), increases with DPPC content (Figure 6c). This is consistent with a slower solvent relaxation as a result of a higher local viscosity.

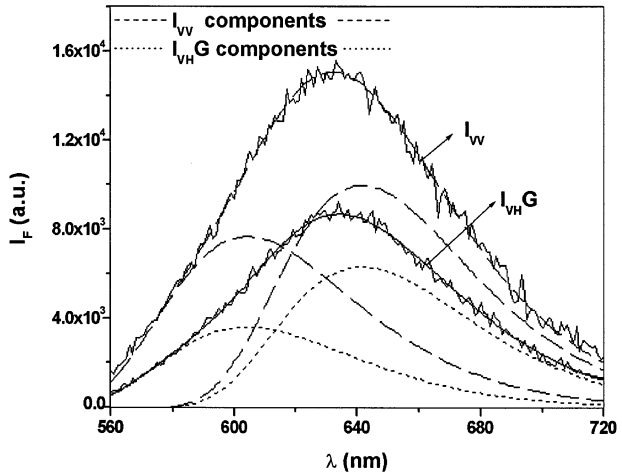

Figure 5. Decomposition of nile red polarized-emission spectra (I_{VV} and GI_{VH}) with two log-normal functions. Fitting curves to experimental results (—), I_{VV} fitting components (– –), and GI_{VH} fitting components (··).

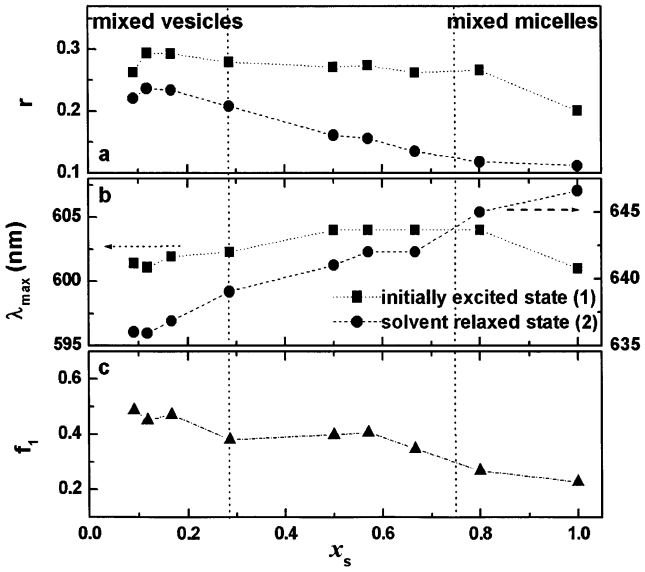

Figure 6. (a) Calculated steady-state anisotropy (eq 6) of the initially excited state (■) and solvent relaxed state (●) of nile red as a function of surfactant molar ratio, x_s. (b) Maximum emission wavelength of the initially excited state (■) and solvent relaxed state (●) as a function of x_s. (c) Emission intensity fraction f_1 of the initially excited state (calculated from eq 7) vs x_s.

Considering the structural changes occurring in these mixed systems, it is observed that the appearance of DPPC-rich structures (mixed vesicles) for $x_s < x_{sol}$ induces a pronounced change in all plotted quantities (r, λ_{max}, and f_1). In the region of mixed-structure coexistence ($x_{sat} < x_s < x_{sol}$), the contribution from the initially excited state is almost constant. In this region, both emitting states have contributions from mixed micelles and mixed vesicles.

The fraction f_1, calculated at the maximum emission wavelength, can be estimated as

$$f_1 = \frac{I_1}{I_1 + I_2} = \frac{n_{mic} n_1^m \alpha_1^m + n_{ves} n_1^v \alpha_1^v}{n_{mic} n_1^m \alpha_1^m + n_{ves} n_1^v \alpha_1^v + n_{mic} n_2^m \alpha_2^m + n_{ves} n_2^v \alpha_2^v} \quad (8)$$

where superscripts v and m indicate mixed vesicles and mixed micelles, respectively; n is the average number of excited molecules per mixed surfactant/lipid aggregate, α is the spectral factor (relating the number of excited molecules to fluorescence intensity), and n_{mic} and n_{ves} are, respectively, the number of mixed micelles and mixed vesicles in the system.

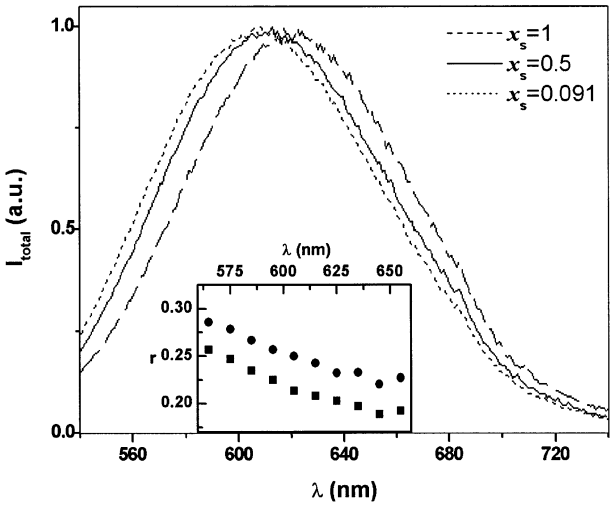

Figure 7. Normalized total-emission spectra ($I_{VV} + 2GI_{VH}$) of DCM for different x_s values (0.091, 0.5, and 1). The inset shows the anisotropy variation with emission wavelength for $x_s = 0.67$ (●) and 1 (■).

This equation can be simplified to

$$f_1 = \frac{f_{mic} n_1^m \alpha_1^m + (1 - f_{mic}) n_1^v \alpha_1^v}{f_{mic}(n_1^m \alpha_1^m + n_2^m \alpha_2^m) + (1 - f_{mic})(n_1^v \alpha_1^v + n_2^v \alpha_2^v)} \quad (9)$$

where f_{mic} is the fraction of mixed micelles in the system.

In this intermediate region ($x_{sat} < x_s < x_{sol}$), the composition of mixed aggregates (vesicles and micelles) remains constant, but the relative proportion of mixed micelles and mixed vesicles is changing. Therefore, only the parameter f_{mic} changes with the surfactant ratio x_s. As can be seen in eq 9, we expect that in f_1 the variation of f_{mic} with x_s is damped.

The anisotropy and λ_{max} of the relaxed state in this intermediate region are not constant, although the local composition is the same. This is explained by the direct influence of f_{mic}. Because the anisotropy is an additive quantity, we have

$$r_2 = f_{mic} r_2^m + (1 - f_{mic} r_2^v) \quad (10)$$

When $x_s < x_{sat}$, only mixed vesicles exist, with a decreasing composition of surfactant as x_s decreases. Nile red relaxed-state emission properties tend to remain constant, indicating that probe molecules are seeing approximately the same environment, probably in the interior of the vesicle bilayer.

DCM Laser Dye in $C_{12}E_7$/DPPC Mixed Systems. Figure 7 displays the normalized total-emission spectra of DCM (obtained from anisotropy measurements) for several x_s values. As for nile red, a blue shift with increasing DPPC content (lower x_s) and a small variation in the spectral bandwidth are also observed.

The inset of Figure 7 shows that the DCM steady-state anisotropy, r, clearly varies with the emission wavelength, decreasing as the emission wavelength increases.

DCM excited-state dynamics involves cis−trans isomerization.[23−27] In the ground state, the main isomer is the trans. It has been found that the environmental properties control the proportion of cis isomer that is formed in the excited state through the photoisomerization process.[23−25] The fraction of cis isomer decreases with the rise in solvent polarity, causing an increase in the fluorescence quantum yield.[23,24] The observed

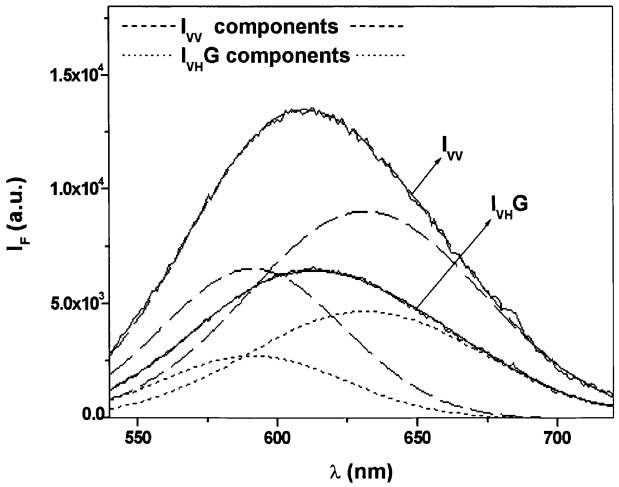

Figure 8. Decomposition of DCM polarized-emission spectra (I_{VV} and GI_{VH}) with two Gaussian functions. Fitting curves to experimental results (—), I_{VV} fitting components (− −), and GI_{VH} fitting components (••) .

variations in fluorescence anisotropy with wavelength can be explained by considering different contributions from the two emitting isomers of DCM.

As for nile red, the emission spectra of DCM were fitted to a sum of two log-normal functions. We found that the skewness parameter ρ always approached 1, which converts the log-normal function into a Gaussian band.

The emission spectra of DCM for the VV and VH combinations of polarizers were then fitted to a sum of two Gaussian functions (eq 4 with $\rho = 1$), keeping the half-width constant for the two emitting isomers (Figure 8).

All of the obtained parameters have the same definitions for nile red, but now subscript 1 refers to the cis isomer (emission on the blue side of the spectrum) and subscript 2 refers to the trans isomer (emission on the red side of the spectrum).

The anisotropy of the cis isomer is greater than that of the trans isomer and more insensitive to the structure and composition of the mixed aggregates (Figure 9a). This is consistent with a published shorter lifetime of the cis isomer,[24] although we expected a smaller solvation volume for the cis isomer than for the trans.

The anisotropy of the trans isomer increases with DPPC content. This is explained by an enhancement of the local viscosity. An increase of the DPPC content causes a slight blue shift of the cis-isomer emission (Figure 9b) without corresponding systematic changes in the trans isomer. The contribution from the cis isomer increases with DPPC content. Although the excited-state dynamics is completely different from that of nile red, the fact that it can also be applied to a two-state model gives DCM approximately the same sensitivity to the structural changes in DPPC/$C_{12}E_7$ mixed systems. One significant difference is that none of the wavelength maxima is significantly sensitive to the DPPC content or to the structure of the mixed aggregates.

Summary and Conclusions

The wavelength dependence of the nile red and DCM anisotropy in mixed DPPC/$C_{12}E_7$ system was successfully described by a two-state model. The obtained variations of the fitted parameters with the surfactant molar ratio are consistent with published data on nile red and DCM excited-state dynamics, taking into account the usually accepted three-stage model of lipid/surfactant interactions. For nile red, the number of

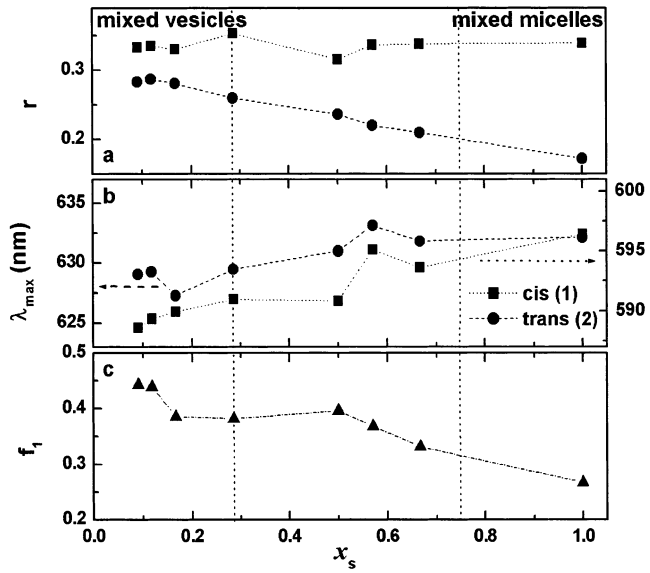

Figure 9. (a) Calculated steady-state anisotropy of the cis (■) and trans isomers (●) of DCM as a function of surfactant molar ratio, x_s. (b) Maximum emission wavelength of the cisr (■) and trans isomers (●) of DCM as a function of x_s. (c) Emission intensity fraction f_1 of the cis isomer (calculated from eq 7) vs x_s.

unrelaxed states rises with DPPC content, which is consistent with an increase in the local viscosity. For DCM, the fraction of cis isomer increases with DPPC content, which agrees with a more favorable trans−cis photoisomerization in a less polar environment. Both probes can be used through wavelength-dependent fluorescence anisotropy to obtain (or confirm) structural information as well as to give some indication of the number of each type of aggregate in these mixed lipid/surfactant microheterogeneous systems.

Acknowledgment. Financial support from the Fundação para a Ciência e a Tecnologia (FCT) under project POCTI/32901/FIS/99 is acknowledged. M.C.R. acknowledges FCT for a grant under the same project.

Note Added after ASAP Posting. This article was released ASAP on 11/16/2002 before all of the author's changes had been incorporated. The correct version was posted on 11/19/2002.

References and Notes

(1) Sujatha, J.; Mishra, A. K. *J. Photochem. Photobiol., A* **1997**, *104*, 173.
(2) Edwards, K.; Almgren, M. *Langmuir* **1992**, *8*, 824.
(3) Miguel, M. G.; Eiddelman, O.; Ollivon, M.; Walter, A. *Biochemistry* **1989**, *28*, 8921.
(4) Edwards, K.; Gustafsson, J.; Almgren, M.; Karlsson, G. *J. Colloid Interface Sci.* **1993**, *161*, 299.
(5) Edwards, K.; Almgren, M. *J. Colloid Interface Sci.* **1991**, *147*, 1.
(6) Inoue, T.; Fukushima, R.; Shimozawa, R. *Bull. Chem. Soc. Jpn.* **1988**, *61*, 1565.
(7) Inoue, T. In *Vesicles;* Rosoff, M., Ed.; Surfactant Science Series; Marcel Dekker: New York, 1996; Vol. 62, pp 151−195.
(8) Duportail, G.; Lianos, P. In *Vesicles;* Rosoff, M., Ed.; Surfactant Science Series; Marcel Dekker: New York, 1996; Vol. 62, pp 295−392.
(9) Greenspan, P.; Fowler, S. D. *J. Lipid Res.* **1985**, *26*, 781.
(10) Mazumdar, M.; Parrack, P. K.; Bhattacharyya, K. *Eur. J. Biochem.* **1992**, *204*, 127.
(11) Sackett, D. L.; Wolff, J. *Anal. Biochem.* **1987**, *167*, 228.
(12) Davis, D. M.; Birch, D. J. S. *J. Fluoresc.* **1996**, *6*, 23.
(13) Maiti, N. C.; Krishna, M. M. G.; Britto, P. J.; Periasamy, N. *J. Phys. Chem. B* **1997**, *101*, 11051.
(14) Datta, A.; Mandal, D.; Pal, S. K.; Bhattacharyya, K. *J. Phys. Chem. B* **1997**, *101*, 10221.

(15) Srivatsavoy, V. J. P. *J. Lumin.* **1999**, *82*, 17.
(16) Hungerford, G.; Castanheira, E. M. S.; Real Oliveira, M. E. C. D.; Miguel, M. G.; Burrows, H. D. *J. Phys. Chem. B* **2002**, *106*, 4061.
(17) (a) Dutt, G. B.; Doriswamy, S.; Periasamy, N. *J. Chem. Phys.* **1991**, *94*, 5360. (b) Dutt, G. B.; Doriswamy, S.; Periasamy, N. *J. Chem. Phys.* **1992**, *96*, 2475.
(18) Deye, J. F.; Berger, T. A.; Anderson, A. G. *Anal. Chem.* **1990**, *62*, 615.
(19) Cser, A.; Nagy, K.; Biczók, L. *Chem. Phys. Lett.* **2002**, *360*, 473.
(20) Hammond, P. R. *Opt. Commun.* **1979**, *29*, 331.
(21) Marason, E. G. *Opt. Commun.* **1981**, *37*, 56.
(22) Antonov, V. S.; Hohla, K. L. *Appl. Phys. B* **1983**, *32*, 9.
(23) Drake, J. M.; Lesiecki, M. L.; Camaioni, D. M. *Chem. Phys. Lett.* **1985**, *113*, 530.
(24) Meyer, M.; Mialocq, J. C.; Rougée, M. *Chem. Phys. Lett.* **1988**, *150*, 484.
(25) Meyer, M.; Mialocq, J. C.; Perly, B. *J. Phys. Chem.* **1990**, *94*, 98.
(26) Easter, D. C.; Baronavski, A. P. *Chem. Phys. Lett.* **1993**, *201*, 153.
(27) Yoshizawa, M.; Kubo, M.; Kurosawa, M. *J. Lumin.* **2000**, *87*−*89*, 739.
(28) Pal, S. K.; Mandal, D.; Sukul, D.; Sen, S.; Bhattacharyya, K. *J. Phys. Chem. B* **2001**, *105*, 1438.
(29) Meguro, K.; Ueno, M.; Esumi, K. Micelle Formation in Aqueous Media. In *Nonionic Surfactants: Physical Chemistry;* Schick, M. J., Ed.; Surfactant Science Series; Marcel Dekker: New York, 1987; Vol. 23, pp 109−183.
(30) Rei, M. C.; Coutinho, P. J. G.; Castanheira, E. M. S., Real Oliveira, M. E. C. D. *Prog. Colloid Polym. Sci.*,in press.
(31) Heerklotz, H.; Binder, H.; Lantzsch, G.; Klose, G.; Blume, A. *J. Phys. Chem. B* **1997**, *101*, 639.
(32) Krishna, M. M. G. *J. Phys. Chem. A* **1999**, *103*, 3589.
(33) Siano, D. B.; Metzler, D. E. *J. Chem. Phys.* **1969**, *51*, 1856.
(34) Shobha, J.; Srinivas, V.; Balasubramanian, D. *J. Phys. Chem.* **1989**, *93*, 17.